Chapter VI

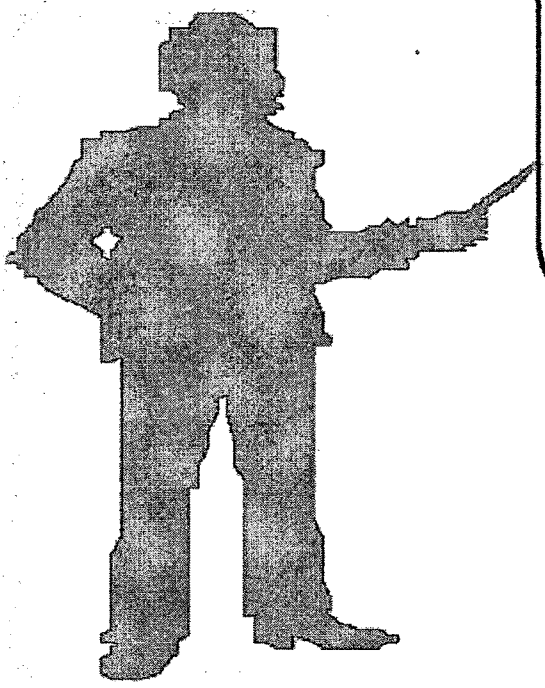

***PolyDOX: In Vivo* Animal Study on EAT Bearing Mice**

6.1. Introduction

A major inherent limitation of current cancer chemotherapy is the non-selectivity of anticancer drugs to tumor cells *in vivo*. Non-specific distribution of anticancer drugs in body after systemic administration, leads to serious side effects on normal cells. Therefore, many research groups are actively working on strategies to improve the biodistribution characteristics, reduce harmful side effects, and enhance favorable pharmacological actions via novel drug delivery formulations which can deliver pharmacologically active drugs to their target sites with high efficiency. To date, bio-conjugates (Banzato et al., 2008; Rosato et al., 2006; Luo et al., 2000), liposomes (Ishida et al., 2009; Elbayoumi et al., 2009; Minko et al., 2006), Solid lipid nanoparticles (Dong et al., 2009; Xu et al., 2009; Jannin et al., 2008; Huynh et al., 2009) and polymeric micelles or nanoparticles (Harada et al., 2006; Nakanishi et al., 2001; Kataoka et al., 2001; Yokoyama et al., 1998) have been developed as carriers for anticancer drugs.

In recent years, liposomal structure resembling novel drug carriers viz polymeric vesicles based on block copolymers have been developed as competent drug carriers, with some remarkable features (Discher and Eisenberg 2002; Levine et al., 2008; Upadhyay et. al. 2009a) and has proved to be an immerging novel carrier for drug delivery (Ahmed et al., 2006; Upadhyay et al., 2009b) and gene therapy (Kim et al., 2009). In previous chapters, we have encapsulated doxorubicin (DOX) in novel polymersomes based on synthesized polypeptide-block-polysaccharide copolymer, namely a poly(γ-benzyl L-glutamate)-block-hyaluronan ($PBLG_{23}$-b-HYA_{10}) and has been addressed as self targeted polymersomes in CD44 expressing cancer cells (Upadhyay et al., 2009b).

Hyaluronan (HYA) is a water soluble, high molecular weight glycosaminoglycan extracellular matrix component essential for proper cell growth and tissue organization. Since this biopolymer is hydrophilic in nature and also major ligand for CD44, a type 1 transmembrane glycoprotein upregulated in certain cancers, it has been used as a long circulating material in blood and also guiding moiety towards tumor which express CD44 receptor *in vitro* and *in vivo* (Peer and Margalit 2004 a, b; Auzenne et al., 2007, Platt and Szoka 2008).

One of the most suitable methods for investigation of *in vivo* behavior of novel drug delivery systems is to label these particles with radionuclides and measure their radioactivity in various tissues and simultaneously perform gamma imaging of the whole body after administration of radiolabeled compound. Now a days, ^{99m}Tc (Technetium) is the choice of scientists among other radionuclide due to easy availability and less radiation burden because of short half life (6h). The ^{99m}Tc is a decay product of [^{99}Mo] molybdate and eluted in the form of [^{99m}Tc] pertechnetate ($^{99m}TcO_4^-$). $^{99m}TcO_4^-$, is negatively charged and chemically nonreactive species. It cannot label to any compound by direct addition. Therefore, it is necessary to reduce Tc (VII) in $^{99m}TcO_4^-$ to a lower oxidation state to produce a stable ^{99m}Tc-nanoparticle complex or to a reactive intermediate complex from which ^{99m}Tc can be easily transferred to a bioactive ^{99m}Tc conjugate (Liu et a., 1997; Vyas et al., 2006). Author's have used ^{99m}Tc as a radioactive tracer for determination of biodistribution, blood clearance and whole body imaging of bioconjugates (Meléndez-Alafort et al., 2006; Banzatoa et al., 2009), nanoparticles (Reddy et al., 2005; Yadav et al., 2007,) and liposomes (Bao et al., 2004; Phillips et al., 1999).

In this study, we aimed to demonstrate *in vivo* efficacy of poly (benzyl L-glutamate)-*block*-hyaluronan (PBLG$_{23}$-*b*-HYA$_{10}$) based polymersomes containing doxorubicin (DOX) as chemotherapeutic agent. We have evaluated the efficacy of DOX loaded polymersomes (PolyDOX) in CD44 receptor expressing Ehrlich Ascites Tumor (EAT) bearing mice. We have also determined the blood kinetics, tissue distribution, side effects and anti tumor efficacy of PolyDOX and compared it with free DOX in normal and EAT bearing mice.

6.2. Materials

^{99m}Tc was freshly eluted from molybdenum for each experiment. Stannous chlorides dehydrate and ascorbic acid was purchased from Sigma Chemicals. Instant thin layer chromatography plates were purchased from Gelman Science Inc. (Ann Arbor, MI). All the other reagents used were of AR grade. Prefiltered (0.2μm filter) distilled water was used in all the studies.

6.3. Radiolabeling of DOX, PolyDOX and Blank polymersomes (Blank-POLY)

The Radiolabeling of free DOX, PolyDOX and blank polymersomes (Blank-POLY) was performed as per published procedure with slight modification (Liu et al., 1997, Reddy et al., 2005 and Meléndez-Alafort et al., 2006). For PolyDOX and Blank-POLY, 25µL stannous chloride (2 mg/mL in 0.1 M Acetic Acid) was added in 100 µL of saline containing pertechnetate ($^{99m}TcO_4^-$) (3mCi; obtained by solvent extraction method from molybdenum). The resulting solution was incubated for 10 min at room temperature (RT), after adjusting the pH to 6.5 with the help of 0.5 M $NaHCO_3$ and so called reduced technetium. PolyDOX (1.0 mg/mL, equivalent to free DOX) and Blank-POLY (1 mg/mL, equivalent to copolymer) were added with reduced technetium and incubated at RT for 30 minutes. In case of free DOX, 25µL of stannous chloride (2 mg/mL in 0.1 M Acetic Acid) and 25µL of ascorbic acid (2 mg/mL) was added in free DOX (1.0 mg/ml) in saline followed by pH adjustment to 6.5 by 0.5 M $NaHCO_3$. To this solution, $^{99m}TcO_4^-$ (3mCi) was added and resulting solution was incubated at RT for 30 minutes. Nitrogen gas was passed to degas all the solutions prior to the mixing or incubation. Labeling efficiency and radiochemical purity (Saha 2004, Harivardhan Reddy et al., 2005, Panwar et al., 2007) was confirmed by ascending instant thin-layer chromatography using silica gel-coated fiber sheets (ITLC-SG) (Gelman Science Inc., Ann Arbor, MI, USA) and 100% acetone was used as mobile phase. ITLC-SG was carried out by running a sample of 2-3µl on a 10 cm strips using acetone as mobile phase. The solvent front was allowed to reach up to a height of about 8 cm from the origin. The strip was cut into two halves (Top and Bottom) and the radioactivity in each half was determined by a well type gamma ray spectrometer (Type GRS23C, Electronics Corporation of India Limited, India). The free pertechnetate (R_f = 0.9–1.0) migrates to the top portion of the ITLC-SG strip, leaving the labeled complex at the bottom. Furthermore, radiochemical purity and labeled efficiency was adjusted by subtracting the migrated activity of unwanted radio colloids in pyridine:acetic acid:water (3:5:1.5). The radio colloids remained at the bottom of the strip, while both the free pertechnetate and the labeled complex migrated with the solvent front. We also measured the particle size after radiolabeling of PolyDOX and Blank-POLY.

$$Free\ ^{99m}Tc\ \% = \frac{T}{T+B} \times 100\%$$

$$\%\ labeling = (100 - \%\ free\ ^{99m}Tc)$$

$$\%\ Purity = (100 - \%\ radio\ colloids)$$

Where T is the counts at top and B is the counts at bottom.

6.4. Transchelation of complexes

In order to check the strength of binding of ^{99m}Tc with the compound, 0.5 ml of the labeled preparation was challenged against various concentrations (10, 30, 50 and 100 mM) of Diethylenetriaminepentaacetic acid (DTPA) (Mishra et al., 2002, Reddy et al., 2005) and incubated for 1 h at 37^{0}C. The effect of DTPA on labeling efficiency was measured on ITLC-SG using acetone as the mobile phase, which allowed the separation of free pertechnetate and DTPA-complex (R_f = 0.8–1.0) from the ^{99m}Tc-DOX, ^{99m}Tc-PolyDOX and ^{99m}Tc-Blank-POLY which remained at the point of application (Rf = 0).

6.5. *In vitro* and *in vivo* stability of radiolabeled compounds

In vitro stability of the radio labelled formulations was monitored in freshly collected human serum and phosphate buffered saline (PBS) (pH =7.4) at 37^{0}C for 48h at 1:1 ratio (50% v/v). At several time points, post incubation (1, 4, 24 and 48 h), samples were analyzed for the radio labeling efficiency using ITLC-SG as described above. In addition, we determined dilution stability of radio labelled compounds. To determine the stability of radio labeled complexes after dilution, 100 µl of complex was diluted to a ratio 1:100 in saline and incubated for 24h at 37^{0}C. The radio labeling efficiency of complex was analyzed by ITLC-SG as described above.

In vivo stability of radio labelled compound was investigated in normal, healthy, female New Zealand rabbits weighing 2.0–2.5 kg. All animal studies were carried out under the guidelines compiled by CPCSEA (Committee for the Purpose of Control and Supervision of Experiments on Animals, Ministry of Culture, Govt. of India) and all the study protocols were approved by Institutional animal ethics committee. ^{99m}Tc (0.5 mCi) (0.5mL injected volume containing 100µg/0.1mL equivalent concentration of DOX) labeled formulations was injected in rabbits through the dorsal ear vein. The blood was

withdrawn through the vein of other ear at different periodic intervals and spotted on the ITLC-SG strips and ITLC-SG carried out as described previously to estimate the possible separation of free ^{99m}Tc.

6.6. Stability study of PolyDOX in serum

Stability of nanoparticles in serum against protein adsorption on the surface of the nanoparticles is an important assay for preclinical study of nanoparticles. Therefore we evaluated the effect of fresh human serum proteins adsorption on the surface of the PolyDOX by measuring the changes in the size of the PolyDOX and Blank-POLY (Han et al., 2006). PolyDOX (1mL) or Blank-POLY (1mL) was added to 1ml of 50% (v/v) serum and the samples were incubated at 37°C with gentle stirring for 48h. After the incubation period, the size of the PolyDOX and Blank-POLY was measured by Zetasizer (Nano ZS, Malvern Instruments Ltd, UK).

6.7. Blood clearance study of ^{99m}Tc-PolyDOX and ^{99m}Tc-DOX

Blood clearance study was performed in normal, healthy, female New Zealand rabbits (n = 3 per group) weighing 2.0-2.5 kg. Animals were injected with 0.5 mCi ^{99m}Tc-labeled formulations (0.5mL injected volume containing 100μg/0.1mL equivalent concentration of DOX) through the dorsal ear vein. The blood samples were withdrawn through the vein of the other ear at different periodic intervals in pre-weighed tubes. The weight of the blood withdrawn at each sampling point was recorded and the radioactivity measured using a well-type γ-ray spectrometer (Type CRS 23C, Electronic Corporation of India Ltd.) along with an injection standard. The activity present in total blood volume was calculated by considering 7.3% of total body weight as total blood weight (Wu et al., 1981, Arulsuda et al., 2004, Agashe et al., 2007). Data were corrected from *in vivo* stability data.

6.8. Expression of CD44 level in EAT cells

Expression of CD44 hyaluronan receptor level in EAT cells were investigated by fluorescence activated cell sorter (FACSCalibur, Becton Dickinson, Germany). EAT cells after rinsing with PBS, 10^5 cells were incubated for 45 min at 4°C with anti CD44-labeled PE antibody (4μg). The stained cells were rinsed twice, collected and

resuspended in 250 μL PBS and the degree of receptor expression was evaluated by flow cytometry.

6.9. Biodistribution on EAT tumor bearing mice

Female BalB/c mice (aged 2 months), weighing between 20 and 25 g were selected for the study. EAT tumor was developed in mice using standard protocol of Dr. A. K. Mishra lab (Division of Cyclotron & Radiopharmaceutical Sciences, INMAS, Delhi, INDIA). Briefly, EAT was maintained in the peritoneum of the mice in the ascites form by serial weekly passage. Exponentially growing EAT cells were harvested, washed, and resuspended in PBS and ~1.0×10^7 cells/mice were injected intramuscularly in the thigh of the left hind leg of the mice. Randomly animals were divided into two groups containing three animals per group. All animals were fasted overnight before the experiment but allowed free access to water. Each of the mice received an injected dose of 100 μCi of the ^{99m}Tc-DOX and PolyDOX (equivalent to DOX 5mg/kg body weight) was administered by the tail vein of each mice. Injected volume of single injection in mice was adjusted as required dose but not more than 10g/0.1mL of mice weight.

The mice were humanely sacrificed at 1, 4, 24 and 48 hours post injection. The blood was collected by the inferior vena cava and subjected to reperfusion with saline to remove blood components from the blood vessels presence in tissues. Subsequently different organs like heart, lungs, liver, kidney, spleen, stomach, intestine, and tissues like muscles and tumor were dissected. The organs and tissues were collected in pre-weighed tubes after washing them with normal saline and drying. Organs and tissues were weighed and radioactivity corresponding to them was measured using well-type γ-scintillation counter along with an injection standard. The percentage of injected dose per gram of tissue (%ID/g) and the liver-to-blood and tumor-to-muscle ratios were calculated.

6.10. Side effects of PolyDOX

Normal mice, 2 months aged were treated with different doses of DOX, PolyDOX and Blank-POLY and observed weight changes and survival time for 25 days from first injection. Mice were randomly divided into 7 groups having 6mice/group and denoted as

DOX (5mg/kg), DOX (15mg/kg), PolyDOX (5mg/kg), PolyDOX (15mg/kg), PolyDOX (20mg/kg), Blank-POLY (20mg/kg) and saline. Dosing schedule was as following -

**DOX (5mg/kg)*	*= single injection on first day*
**DOX (15mg/kg)*	*= daily injection (5mg) for 3 days (total dose 15mg/kg)*
**PolyDOX (5mg/kg)*	*= single injection on first day*
**PolyDOX (15mg/kg)*	*= daily injection (5mg) for 3 days (total dose 15mg/kg)*
**PolyDOX (20mg/kg)*	*= daily injection (5mg) for 4 days (total dose 20mg/kg)*
**Blank-POLY (20mg/kg)*	*= single injection on first day*
**Saline*	*= single injection on first day*

Furthermore, we determined hematological parameters, serum biochemical analysis and histopathology of treated normal mice organs against control mice (saline treated). Mice were randomly divided in 13 groups and each group was having 3 animals. Dosing was as per above mentioned schedule. These 13 groups were further divided into 2 groups (A & B). A and B represents blood samples collection on 7^{th} and 21^{st} day after last injection by cardiac puncture and animals were sacrificed for histopathological examination of organs. All formulations were administered by IV route and blood samples was collected in heparin tubes (LABTECH Disposables, INDIA) and given for hematology analysis and serum analysis to Pathology Laboratory (Dr Lal PathLabs, Delhi, INDIA).

Following organs and tissue were dissected for further histopathological analysis: heart, spleen, liver, lungs, kidney, stomach, intestine, muscles and tumor. Tissue samples were prepared in Lab (Singh Histology Processing Centre, New Delhi, INDIA) as per their standard protocol. Briefly, sample was fixed for 3 h in 4% paraformaldehyde (BDH, INDIA) and washed extensively with PBS overnight. Tissues were paraffin embedded (BDH, INDIA) and sections were cut at 4 μm thickness. Sections were de-paraffinised and dehydrated in xylene and ethanol (Sigma, INDIA) and stained with hematoxylin and eosin (Sigma, INDIA) to assess histological alterations using a microscope (Olympus BX60, JAPAN) at 20×Magnification.

6.11. Hemolysis activity of PolyDOX

The hemolysis test was conducted as described by Shuai et al., 2004 with slightly modifications. Fresh human blood (healthy 30 year old, type B positive male with normal blood chemistry) collected in heparin tubes (LABTECH Disposables, INDIA) from pathology lab. In brief, blood was washed three times with PBS and red blood cells (RBCs) were collected by centrifugation at 2800 rpm for 5 min. The washing step was repeated in order to remove debris and serum protein. The PolyDOX at different concentrations varying from 50 to 200µg/mL and Blank-POLY from 50 to 500µg/mL were used for experiment. Typically, 100 µl of the erythrocyte suspension was added to 900 µl of formulations. The samples were incubated for 60 min at 37^0C in incubator with intermittent shaking. The release of hemoglobin was measured by visible spectrophotometric analysis of the supernatant at 540 nm after centrifugation at 3000rpm for 60 minutes. Erythrocytes incubated with saline and distilled water served as negative (0%) and positive controls (100%), respectively and all hemolysis data points are presented as the percentage of the complete hemolysis. The results of the hemoglobin assay was adjusted by subtraction of the absorbance of the no-blood control (i.e., sample containing all assay components except the blood is substituted by PBS) (Dobrovolskaia et al., 2008). The % hemolysis rate (%HR) was calculated from the following equation.

$$\% HR = \frac{A_t - A_{nc}}{A_{pc} - A_{nc}} \times 100$$

Where A_t, A_{nc}, and A_{pc} are the absorbance of the tested sample, the negative control, and the positive control, respectively. The experiments were run in triplicate.

6.12. Antitumor activity of PolyDOX

The *in vivo* antitumor efficacy of the PolyDOX was assessed in female BalB/c mice (body weight = 20 to 25 g). EAT tumor was developed as per above mentioned procedure. Randomly animals were divided into three groups (Control, free DOX and PolyDOX) and each group was having six mice. Mice were treated with a single intravenous injection of 5 mg/kg body weight dose equivalent to DOX in each group. The control group mice received a single intravenous injection of saline. At predetermined time intervals, tumor volume was determined by measuring its dimensions using a digital

caliper and calculated as per below mentioned formula. Throughout the experiments, all animals were accommodated in a pathogen-free laboratory environment. The study was terminated after 30 days post treatments.

$$Tumor\ Volume\ (mm^3) = width \times length^2/2$$

In addition, tumor volume doubling time (DT) was calculated with the following equation (Devalapally et al., 2007).

$$DT = \frac{T \times log2}{(\log V_F - \log V_i)}$$

Where V_F is the final tumor volume, V_i is the initial tumor volume at drug treatment time-point, and T is the time difference between the initial and final day.

Survival observation of treated tumor bearing mice was continued till tumor volume reached 50% above the ethical limit (2000mm^3) (Greeneltch et al., 2007) or death occurred after post treatments. Whichever first observed was counted as death. We also calculated Increase in Life Span (ILS) (Wang et al., 2000) from the survival data as per below mentioned formula.

$$ILS\ (\%) = (T/C\text{-}1) \times 100$$

Where T and C are the mean survival time of treated mice and control mice.

6.13. Gamma Scintigraphy study of PolyDOX

Gamma Scintigraphy study was performed in mice after intravenously administering (100μCi) of ^{99m}Tc-PolyDOX containing 5mg/kg dose equivalent to DOX. The animals were anaesthetized using chloroform and mounted on a wooden board. The imaging was performed on single photon emission computerized tomography (SPECT, LC 75-005, Diacam, Siemens, Hoffman Estates, IL, USA) at different time intervals (1h, 4h and 6h).

6.14. Statistical analysis

All data expressed as means ± standard deviation (S.D.) are representative of at least three or six different experiments. When comparing more than two mean values of groups, a one-way analysis of variance (ANOVA) was performed using KaleidaGraph (Version 4.01) program. To find out whether the two values of interest were significantly

different, Post Hoc Test was performed. Difference between two groups was evaluated using Student's t-test. A "P" value less than 0.05 was considered statistically significant.

6.15. Results and Discussion

6.15.1. ^{99m}TC labelled PolyDOX, Blank-POLY and free DOX

^{99m}Tc radionuclide was used to investigate *in vivo* behavior of novel self targeted polymersomes due to easy availability, cost effectiveness and low radiation dose. Since half-life of ^{99m}Tc is 6h as compared to commonly used radionuclides such as for ^{125}I, 60 days; ^{14}C, 5730 years; ^{3}H, 12.33 years therefore it presents less radiation burden. ^{99m}TC radionuclide is the decay product of Molybdenum and is present in higher oxidation state (+7). In higher oxidation state, it cannot be directly labeled with compound therefore we used stannous chloride dehydrate to reduce $^{99m}TcO_4^-$ from +7 oxidation state to lower oxidation state (+4). Reduced ^{99m}Tc directly labeled PolyDOX and Blank-POLY whereas ascorbic acid was used in case of free DOX to achieve higher labeling efficiency. This process was optimized to get minimum impurities (free $^{99m}TcO_4^-$, and radio colloids). Figure 6.1 represents ^{99m}Tc labeling efficiency of the compounds. All compounds were labelled with ^{99m}Tc by direct labeling method and represent more than 99% labeling efficiency together with less than 1% impurities (free $^{99m}TcO_4^-$, and radio colloids). There was no significant difference in particle size of PolyDOX and Blank-POLY after ^{99m}Tc labeling.

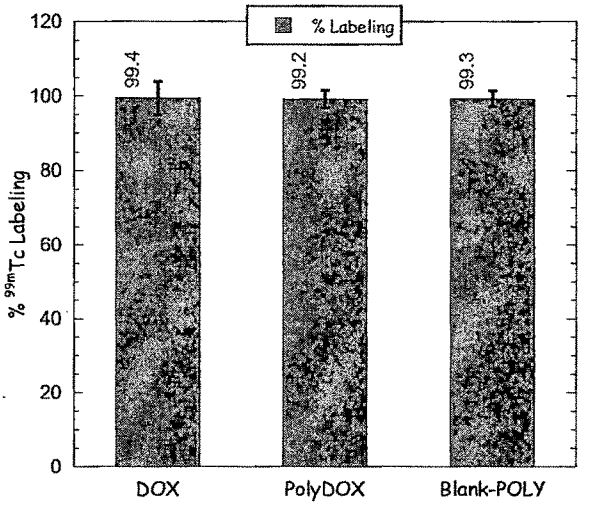

Figure 6.1 ^{99m}Tc Radiolabeling efficiency of DOX, PolyDOX and Blank-POLY.

Binding strength of labelled compounds was determined with DTPA challenge. Challenge study demonstrated that the labeling efficiency of the complexes was not considerable affected in presence of DTPA even at higher concentration (100mM) (Table 6.1) and indicated strong and stable complex between ^{99m}Tc and used compounds.

The *in vitro* stability of the labeled formulations was evaluated in PBS (pH = 7.4) and in human serum and is represented in Table 6.2. The *in vitro* stability was determined up to 48h. The data demonstrated excellent stability of the labeled complexes in PBS and serum up to 48h as indicated by their labeling efficiency (Table 6.2). Labeling efficiency was more than 98% in PBS and more than 86% in presence of serum at 37^{0}C after 48h. Stability of ^{99m}Tc-PolyDOX and ^{99m}Tc-Blank-POLY was ~90% at 100 times dilution after incubation for 24h at 37^{0}C and for ^{99m}Tc-DOX was ~85% (Table 6.3).

In addition, we observed good stability of the radio labelled compounds *in vivo* at different time points (Table 6.4). PolyDOX and Blank-POLY contain hydroxyl and carboxyl groups on the surface due to hyaluronan presence, which can coordinate with metal core and produce stable radio labeled complex (Meléndez-Alafort et al., 2006). This could be the explanation of their good stability *in vitro* and *in vivo*. Above mentioned *in vitro* and *in vivo* stability data suggests that ^{99m}Tc radio nucleotide could be ideal radio tracer as markers for the *in vivo* application in our study.

Table 6.1 *In vitro* stability of ^{99m}Tc-labelled compound in presence of DTPA (n =3)

% Transchelation with DTPA			
Conc.(mM)	DOX	PolyDOX	Blank-POLY
10	1.29±0.11	ND	ND
30	1.87±0.09	1.13±0.06	1.27±0.06
50	2.91±0.18	1.39±0.11	1.92±0.13
100	9.69±0.67	5.52±0.36	4.84±0.19

Table 6.2 *In vitro* stability of ^{99m}Tc-labelled compounds in PBS and serum (n =3)

Post incubation time (h)	PBS			Serum		
	DOX	PolyDOX	Blank-POLY	DOX	PolyDOX	Blank-POLY
1	99.41±4.48	99.17±2.41	99.27±2.12	99.21±4.49	99.59±3.28	99.46±3.47
4	99.74±2.97	98.38±1.96	98.15±2.73	97.58±3.71	98.11±3.48	98.51±2.91
24	98.37±3.62	97.08±2.83	97.94±3.08	88.39±2.93	94.47±3.17	96.34±2.57
48	98.64±2.81	98.53±3.68	98.15±2.42	86.24±3.52	91.81±2.92	92.18±2.63

Table 6.3 *In vitro* stability after 100 times dilution of ^{99m}Tc-labeled compounds (n =3)

Incubation time (h)	DOX	PolyDOX	Blank Polymersome
0	99.28±7.9	99.51±6.31	99.42±5.92
2	97.49±8.1	98.03±4.72	98.81±7.37
5	92.62±5.22	97.82±6.18	97.21±5.82
24	85.72±6.02	89.94±4.27	90.19±3.79

Table 6.4 *In vivo* stability of ^{99m}Tc-labeled compounds (n =3)

Sampling time (h)	DOX	PolyDOX	Blank Polymersome
1	99.97±5.82	99.20±4.91	99.74±3.71
4	97.71±6.47	97.90±5.28	98.41±6.97
24	89.19±4.99	90.05±4.63	91.85±2.01
48	86.67±4.71	88.60±2.92	88.02±6.11

6.15.2. *Stability of PolyDOX and Blank-POLY in serum*

Particle sizes of PolyDOX and Blank-POLY did not change after incubation with human serum for 48h at 37°C (Figure 6.2). These results indicate that hydrophilic surface of PolyDOX and Blank-POLY can reduce the interactions with plasma proteins, might be due to high flexibility and hydrophilicity of the hyaluronan present on the surface.

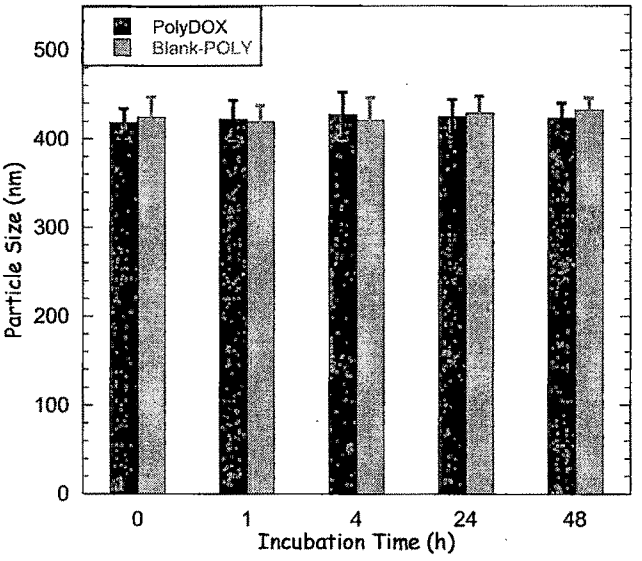

Figure 6.2 Stability of PolyDOX and Blank-POLY in human serum at 37^{0}C for 48h. The data represent the mean ± S.D (n = 3).

6.15.3. *Blood Clearance study of ^{99m}TC labeled compounds*

The profiles of the DOX concentration in the bloodstream are shown in figure 6.3 after the IV injection of ^{99m}Tc-labeled compounds (free DOX, PolyDOX and Blank-POLY).

All the ^{99m}Tc-labeled compounds were rapidly cleared from the blood circulation. However, there was significant difference ($P<0.01$) in plasma profile between the injected ^{99m}Tc-labeled compounds. PolyDOX concentration was significantly higher ($P<0.001$) in bloodstream than that of free DOX at each sampling time points whereas no significant difference ($P>0.05$) was found between PolyDOX and Blank-POLY.

Non-compartmental pharmacokinetic analysis was performed using AUC+ method in Kinetica-4.4 (InnaPhase Corp, Philadelphia, PA, USA) for IV bolus. The area under the plasma concentration-time curve (AUC) was calculated by using the linear trapezoidal method. The terminal elimination rate constant (lz) was estimated from the slope of the terminal phase of the log plasma concentration-time points fitted by the method of least-squares, and then the terminal elimination half-life ($T_{1/2}$) was calculated as 0.693/lz. The values of apparent volume of distribution during the terminal phase (Vz) and apparent volume of the plasma compartment (Vss) were directly derived from software. The total

clearance (CL) was calculated as $0.693*Vz/T_{1/2}$. All pharmacokinetic parameters are presented in Table 6.5.

The PolyDOX significantly increased the half-life ($T_{1/2}$; 19.48h), mean residence time (MRT; 24.72h) and area under the curve (AUC; 59.61% h/mL) of DOX in circulation, as compared with free DOX ($T_{1/2}$; 5.54h, MRT; 6.99h, AUC; 24.26% h/ml). These results indicate that PolyDOX can circulate for a longer time in the blood circulation system than free DOX.

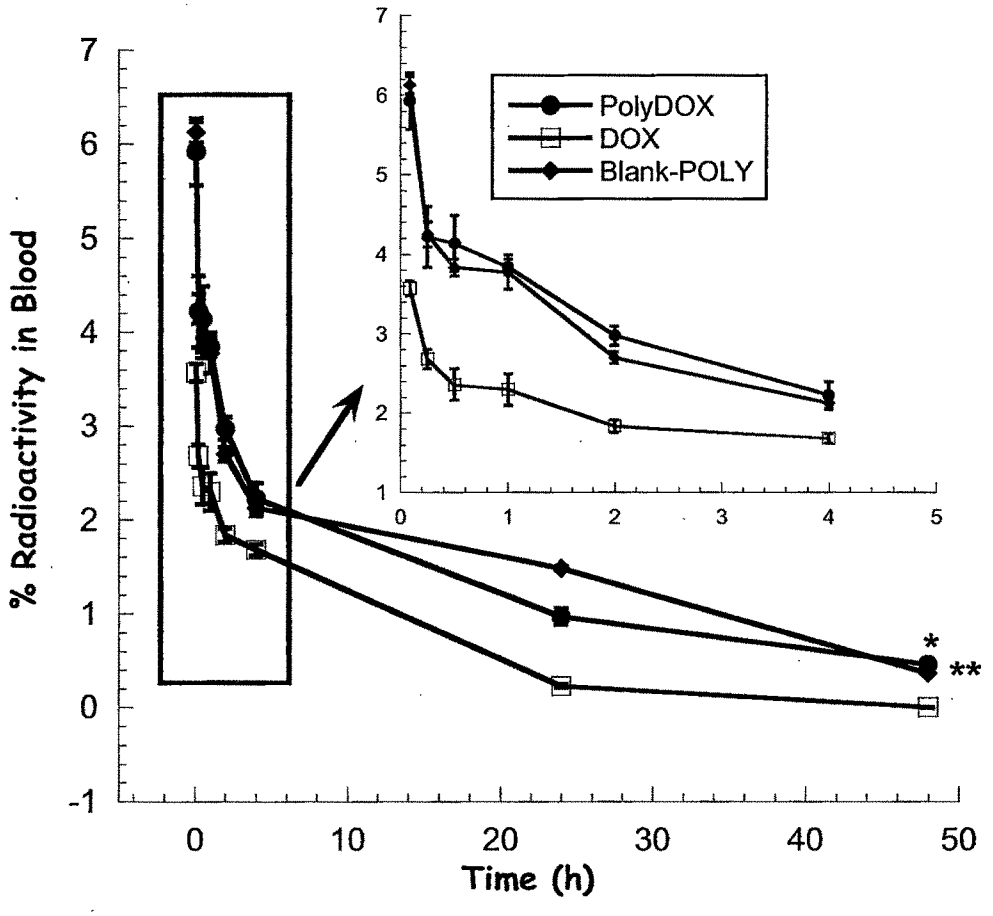

Figure 6.3 Pharmacokinetic profiles of DOX, PolyDOX, and Blank-POLY after single intravenous injection in rabbit. *P < 0.001 (PolyDOX vs. DOX), **P > 0.05 (PolyDOX vs. Blank-POLY).The data represent the mean ± S.D (n = 3).

Table 6.5 Pharmacokinetic parameters of ^{99m}Tc-Labeled compounds in rabbits (n =3)

Pharmacokinetic Parameters	DOX	PolyDOX*	Blank Polymersome
C_{max} (%)	3.57	5.92	6.13
T_{max} (h)	0.083	0.083	0.083
AUC_{0-48} (%h/mL)	24.26	59.61	67.20
$T_{1/2}$ (h)	5.54	19.48	15.54
MRT(h)	6.99	24.72	22.74
Lz (h^{-1})	0.125	0.0356	0.0445
CL (%/h)	0.805	0.798	0.843
Vz (mL)	6.438	22.43	18.91
Vss (mL)	5.628	19.72	18.35

*$p<0.001$ vs. DOX

Above mention results suggest that hyaluronan stabilized polymersomes can prolong the blood circulation time of DOX after IV administration. Remarkably, presence of hydrophilic surface due to hyaluronan on the PolyDOX protected DOX from the serum proteins and prolonged its half-life as compared with those of the free DOX. Hyaluronan has been reported as hydrophilic material for coating on liposome for enhancement of long circulating time compare to PEGylated liposome (Doxil) in healthy and tumor bearing mice (Peer and Margalit 2004b).

6.15.4. *Ehrlich Ascites Tumor*

In our study, we used Ehrlich Ascites Tumor model for *in vivo* studies. Ehrlich Ascites Tumor is a transplantable tumor that arises from a mouse mammary adenocarcinoma. It grows in both ascitic and solid forms (Ferreira et al., 2007). We have already shown the self targetable property of PolyDOX towards CD44 receptor expressing cancer cells (Chapter V; Upadhyay et al., 2009b). Therefore we have determined the CD44 receptor expression level in EAT cells after incubating with anti CD44 antibody. It is clear from figure 6.4 that EAT cells significantly express CD44 level and it could be the good model for investigation of *in vivo* behavior of PolyDOX.

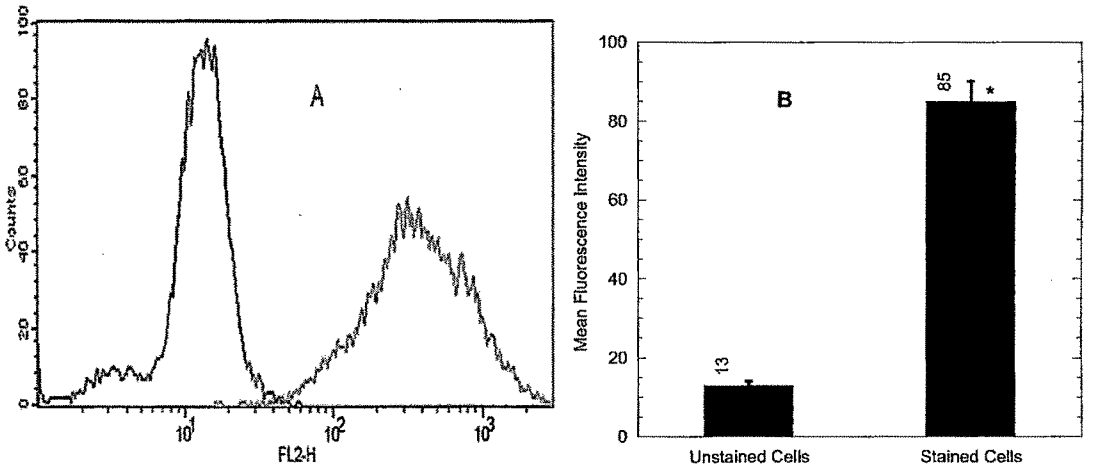

Figure 6.4 (A) CD44 expression on Ehrlich Ascites Tumor (EAT) cells measured by flow cytometry. Black and Grey lines are representing unstained and stained cells with PE labeled CD44 antibody respectively. (B) Mean fluorescence intensity of unstained and stained cells (EAT) measured by flow cytometry. (n = 3, * P<0.001 vs. unstained cells).

6.15.5. *Biodistribution study of ^{99m}Tc-labelled compounds*

Biodistribution pattern of ^{99m}Tc-PolyDOX and free ^{99m}Tc-DOX were investigated in EAT bearing mice with 5mg/kg body weight dose equivalent to DOX. Figure 6.5 represents complete tissue distribution after intravenous administration of ^{99m}Tc-labeled compounds (PolyDOX and free DOX) and results expressed in ^{99m}Tc-labeled compounds (DOX and PolyDOX) accumulated per gram of tissue (expressed as percentage of the injected dose/g tissue, %ID/g) at different time intervals. Tissue uptake of PolyDOX was significant (P<0.01) in each organs than free DOX.

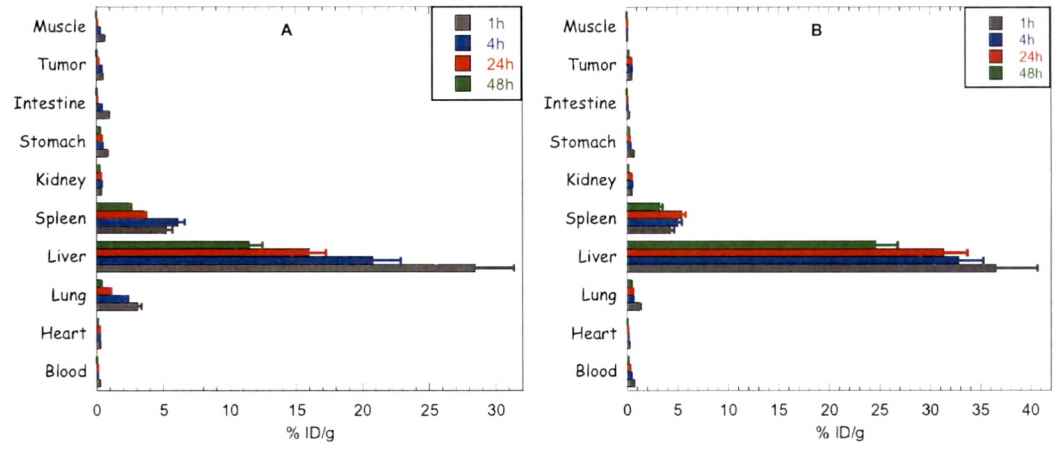

Figure 6.5 (A) Complete tissue distribution of ^{99m}Tc-DOX and (B) for ^{99m}Tc-PolyDOX after intravenous injection in BalB/c mice at a single dose of 5 mg/kg. Each point represents the mean of three mice ±S.D.

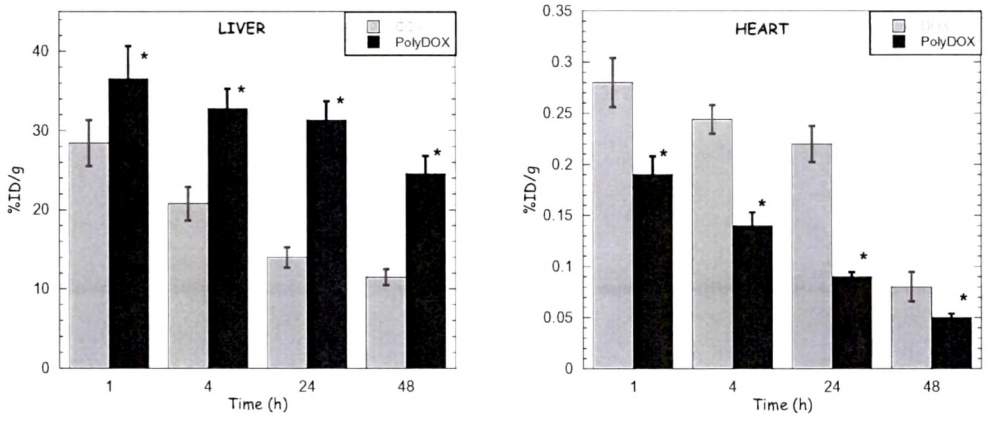

Figure 6.6 Liver and Heart tissues uptake of ^{99m}Tc-DOX and ^{99m}Tc-PolyDOX. (*P<0.001 vs. DOX).

Results showed the liver > spleen > lungs to be the organs of preferential accumulation of ^{99m}Tc-PolyDOX. After 1h, 36.54 % ± 4.13, 4.31% ± 0.372 and 1.24% ± 0.11 of the injected activity was accumulated in the liver, spleen and lungs, respectively. However free DOX uptake is also more after 1h in liver > spleen > lungs (28.45±2.9 > 5.23±0.491 > 3.084±0.278 respectively). PolyDOX uptake was significantly high (P<0.01) in liver and low (P<0.01) in heart compared to free DOX (Figure 6.6).

Peer and Margalit had reported similar results and obtained higher uptake of DOX in liver > spleen after intravenous injection of hyaluronan coated liposome encapsulated DOX in B16F10.9 tumor-bearing C57BL/6 mice (Peer and Margalit 2004b). Hyaluronan

uptake in liver and spleen is mediated by presence of Hyaluronan Receptor for Endocytosis (HARE) and increases as molecular weight increase (Zhou et al., 2000; Sugahara et al., 2001; Harris et al., 2007). ^{99m}Tc labeled hyaluronan-paclitaxel bioconjugate (^{99m}Tc-ONCOFID-P) was approximately 80 % and 6 % of the injected activity was accumulated in the liver and spleen respectively (Meléndez-Alafort et al., 2006, Banzatoa et al., 2009). Similar tissue distribution results were also found after intravenous administration of hyaluronic acid esterified with butyric acid and labelled with technetium-99m (^{99m}Tc-HA-But) (Coradini et al., 2004). Besides HARE receptor, research has shown that particles with hydrodynamic radii of over 200 nm typically exhibit a more rapid rate of removal by liver and spleen than particles with radii under 200 nm, regardless of whether they are PEGylated or not (Moghimi et al., 1993). In our case, we performed study on ~400nm particle size. Therefore, above mentioned reason could be also explanation of removal of PolyDOX by liver and spleen.

We had determined the liver/blood ratio of ^{99m}Tc-DOX and ^{99m}Tc-PolyDOX and are shown in figure 6.7A. PolyDOX reduce significantly ($P<0.05$) the ratio between liver/blood than DOX which indicate PolyDOX clearance was delayed compared to free DOX after IV injection of PolyDOX. After 1h, tumor uptake of free DOX was significant ($P <0.01$) but later on PolyDOX uptake was increased significantly ($P <0.001$) compared to free DOX (Figure 6.8). At 48h, free DOX uptake was 0.02% ± 0.0014 whereas PolyDOX uptake was 0.16% ± 0.011. In addition, we also determined ratio of uptake of free DOX and PolyDOX between tumor and muscle (opposite side than tumor) (Figure 6.7B). Interestingly, PolyDOX showed high ratio of uptake between tumor and muscles and was significantly higher than free DOX ($P <0.001$).

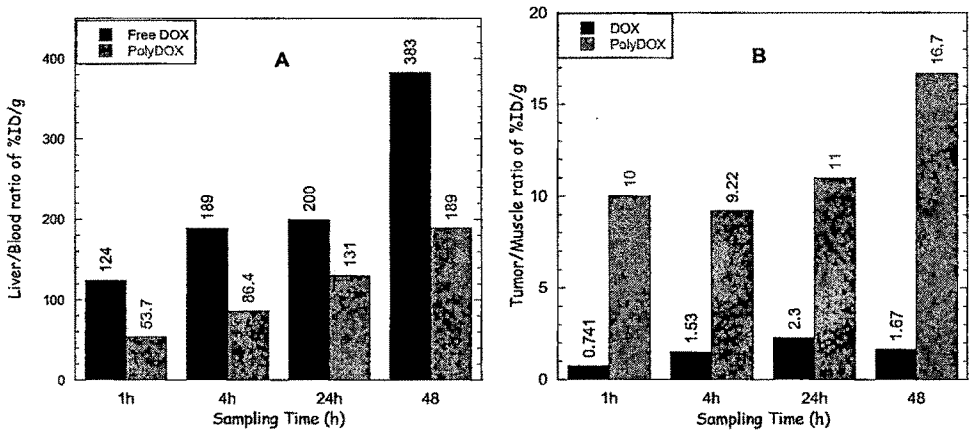

Figure 6.7 (A) Liver/Blood uptake ratio (P<0.05, PolyDOX vs. DOX) and (B) Tumor/Muscle uptake ratio (P<0.001, PolyDOX vs. DOX).

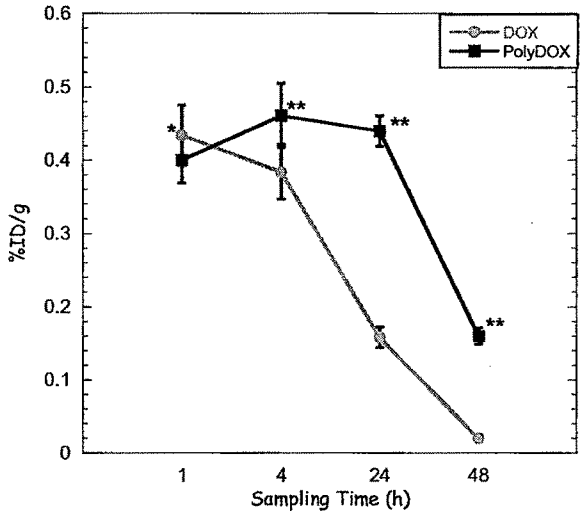

Figure 6.8 Tumor uptakes of DOX and PolyDOX after intravenous injection in BalB/c mice at a single dose of 5 mg/kg. Each point represents the mean three mice ±S.D. (n = 3). (*P<0.001 vs. PolyDOX and **P<0.001 vs. DOX)

Notably, PolyDOX concentration was found lower and significant (p<0.001) in the heart at all time points (Figure 6.6). DOX induces reactive oxygen species (ROS) which produce DOX mediated cardiac toxicity (Ito et al., 2009) and presence of free DOX in heart is closely related to the inherent cardiac toxicity of DOX. We have already seen that PolyDOX reduces serum enzymes (CPK and LDH) level which is induced by free DOX and are indicator for cardiac toxicity (Chapter V). Therefore using PolyDOX formulation, could reduce cardiac toxicity of free DOX because of low uptake and also control release

behavior of PolyDOX *in vitro* which allows control release of DOX (Upadhyay et al, 2009; Chapter IV).

6.15.6. Toxicity of PolyDOX

It was of interest to assess the biocompatibility or toxicity of these compounds *in vivo* to prove the safety of PolyDOX as a novel drug carrier therefore we evaluated toxicity for PolyDOX *in vivo* after single and multiple injections through the lateral tail vein at different doses of DOX. During the course of experiment, we observed change in body weights of mice (Figure 6.9). The overall body weight change was in the following order: DOX, 15 mg/kg (3×5mg/kg/day) > DOX, 5 mg/kg > PolyDOX, 20mg/kg (4×5mg/kg/day) > PolyDOX, 15mg/kg (3×5mg/kg/day) > PolyDOX, 5mg/kg > Blank-POLY (20mg/kg) > Control (Saline); and values ranged between -6.0% and +11% for all groups (Table 6.6). Significant weight loss ($p<0.001$) was observed in DOX treated mice compared to control, Blank-POLY and PolyDOX treated mice.

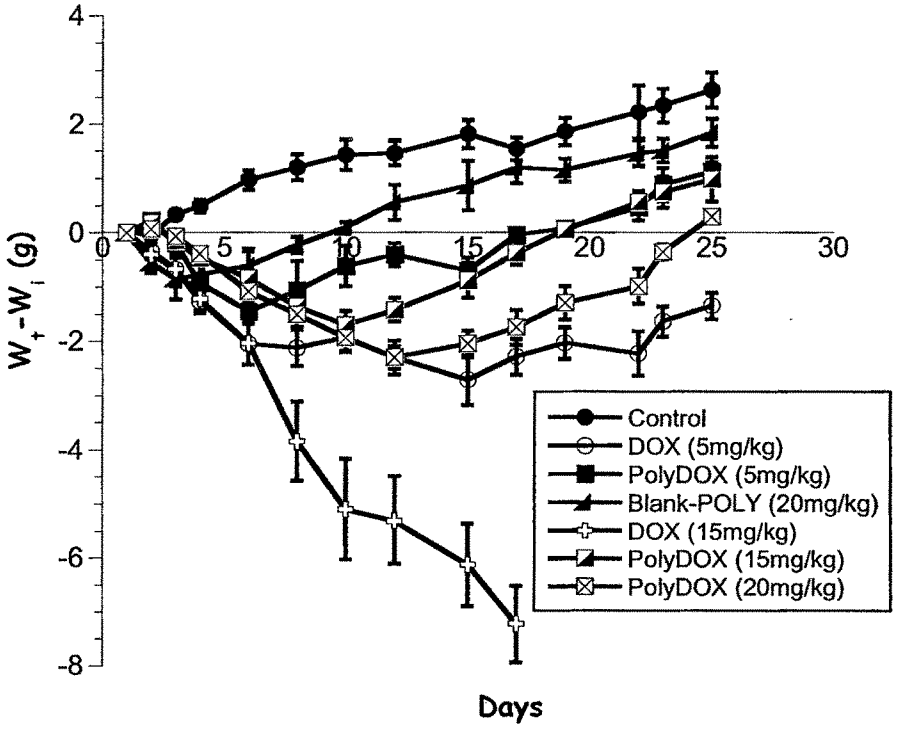

Figure 6.9 Weight changes in healthy BalB/c mice after IV administration of DOX, PolyDOX and Blank-POLY. W_t and W_i is the weight of treated animal and animal weight on initial day respectively. Each point represents the mean of six mice ±SD.

Table 6.6 Body weight changes in treated mice at different doses of DOX, PolyDOX and Blank-POLY after 25 days from first injection

Sample	Dose (mg/kg)[a]	Body weight change on 25th day (%)	Toxic death
Control	0	11.12±0.83	0/6
Blank-POLY	20	7.80±0.91	0/6
DOX	5	-5.95±0.47*	0/6
-	15	-	6/6
PolyDOX	5	4.71±0.52	0/6
-	15	4.44±0.29	0/6
-	20	1.29±0.21	0/6

[a] Dose administration was single injection and multiple injection (total injected dose). (*P<0.001, significant difference as compared to other treated groups).

Animals receiving a total dose 20 mg/kg PolyDOX when administered by four injections (4×5mg/kg/day), or 15mg/kg by three injection (3×5mg/kg/day), or 5mg/kg by single injection and free DOX (5mg/kg) injected as single dose, showed extended survival for more than a month compared with animals receiving a total dose of 15 mg/kg free DOX administered by 3 injections (3×5mg/kg/day); all mice receiving free DOX (15mg/kg) died within 17days from first injection. This can be correlated to LD_{50} (lethal dose killing 50% of the test animals) of DOX, is generally 12.7-13.2 mg/kg (Bae et al., 2005). In addition, Blank-POLY at single dose (20mg/kg) had not affected survival time of treated mice (Table 6.6).

Blood analyses were performed at 7 and 21 days after the end of the day from last IV injection of different doses of DOX, PolyDOX and Blank-POLY in healthy mice (3mice/group). No considerable difference in blood parameters was observed after treatment with PolyDOX (5, 15, 20 mg/kg) and with Blank-POLY (20mg/kg) (Table 6.7, 6.8). Specifically, there was no considerable difference in RBC counts, in peripheral WBC count and platelet counts remained adequate at both time points tested (Table 6.7, 6.8) compared to control. In contrast, free DOX received animals showed considerable differences from the control group (Table 6.7, 6.8) for WBC, Platelets counts and lymphocytes. Similar side effect was observed at dose 10mg/kg of DOX (Greish et al., 2004).

Table 6.7 Blood parameters in healthy mice on day 7 after last intravenous doses of PolyDOX injections (5mg/kg/day), (4×5mg/kg/day), (3×5mg/kg/day), free DOX injection (3×5mg/kg/day), (5mg/kg/day) and Polymersomes (20mg/kg/day)

Parameter (Units)	Untreated (Control)	DOX (5mg/kg)	PolyDOX (5mg/kg)	Bank-POLY (20mg/kg)	DOX[a] (15mg/kg)	PolyDOX (15mg/kg)	PolyDOX (20mg/kg)
Haemoglobin (g/dL)	15.3±0.09	13.18±1.1	14.71±0.8	14.69±1.2	11.97±1.1	13.84±0.6	13.57±1.2
Packed Cell Volume (%)	42.0±3.6	43.1±2.4	43.52±4.1	42.16±3.7	45.73±3.2	43.3±4.1	44.2±4.5
Leukocyte Count, Total (thou/mm^3)	7.5±0.45	4.1±0.38	6.9±0.64	8.1±0.71	3.2±0.29	5.7±0.52	5.6±0.4.9
RBC Count (mill/ mm^3)	9.78±0.94	8.83±0.47	9.7±0.91	9.24±0.82	7.53±0.63	9.61±0.91	10.27±0.84
MCV (fL)	47.8±3.2	47.39±4.2	47.11±2.9	47.9±3.82	47.3±4.12	47.2±4.14	47.1±3.75
MCH (pg)	15.40±1.3	15.28±0.91	15.4±1.1	15.97±1.4	14.63±1.1	15.41±0.97	15.62±1.3
MCHC (g/dL)	32.94±2.4	31.0±1.9	32.5±2.7	33.8±2.6	32.21±1.9	31.4±2.1	31.9±3.1
Platelet Count (thou/mm^3)	975±94	821±75	934±86	1020±79	736±59	942±72	959±42
Lymphocytes (thou/mm^3)	2.17±0.24	1.72±0.19	2.28±0.24	2.31±0.19	1.97±0.22	2.04±0.34	2.4±0.21
Monocytes (thou/mm^3)	0.23±0.01	0.17±0.02	0.34±0.02	0.29±0.04	0.26±0.02	0.31±0.04	0.29±0.02

[a]This experiment was performed on two mice because one animal died before 7 days. Red Blood Cell (RBC), Mean Corpuscular Volume (MCV), Mean Corpuscular Hemoglobin (MCH), Mean Corpuscular Hemoglobin Concentration.

Table 6.8 Blood parameters in healthy mice on day 21 after last intravenous doses of PolyDOX injections (5mg/kg/day), (4×5mg/kg/day), (3×5mg/kg/day), free DOX injection, (5mg/kg/day) and Polymersomes (20mg/kg/day)

Parameter (Units)	Untreated (Control)	DOX (5mg/kg)	PolyDOX (5mg/kg)	Polymersomes (20mg/kg)	PolyDOX (15mg/kg)	PolyDOX (20mg/kg)
Haemoglobin (g/dL)	14.8±1.2	13.79±0.97	14.2±1.2	15.1±1.3	14.26±1.2	15.44±1.4
Packed Cell Volume (%)	40 ±2.6	44.7±3.9	41.37±2.1	42.11±2	42.9±3.4	4.4±3.6
Leukocyte Count, Total (thou/mm^3)	8.1±0.64	5.8±0.41	7.4±0.59	8.4±0.63	6.2±0.44	6.9±7.1
RBC Count (mill/ mm^3)	9.14±0.86	10.21±0.83	9.49±0.84	8.99±0.87	10.52±0.42	9.83±6.3
MCV (fL)	48.14±2.7	49.11±3.1	48.72±4.2	47.64±3.49	47.92±3.71	48.46±2.45
MCH (pg)	14.85±1.1	13.81±1.4	15.13±0.98	14.58±1.2	14.63±1.1	14.47±1.4
MCHC (g/dL)	31.86±3.2	32.47±2.2	32.71±3.1	32.86±2.4	32.6±3.22	32.76±2.6
Platelet Count (thou/mm^3)	921±62	792±54	979±48	961±52	849±35	821±73
Lymphocytes (thou/mm^3)	2.67±0.27	1.79±0.11	2.12±0.15	2.84±0.25	2.12±0.18	2.24±0.27
Monocytes (thou/mm^3)	0.49±0.02	0.26±0.01	0.36±0.03	0.38±0.02	0.27±0.03	0.36±0.04

Serum was separated from the blood collected from treated mice and was investigated for blood biochemical analysis (Table 6.9). It is noteworthy that the levels of CPK (creatine phosphokinase), LDH, (lactate dehydrogenase), aminotransferases (ALT and AST) and creatinine and BUN were normal in groups treated with PolyDOX (5, 15 20 mg/kg) and with Blank-POLY (20mg/kg), indicating that the heart, liver and renal functions were normal. However, mice treated with free DOX (5 and 15mg/kg) showed considerable difference in level of serum enzymes compared to control. It has been reported that free DOX at 10mg/kg increase significantly CPK, LDH and AST serum enzymes in ddY mice (Greish et al., 2004).

Histopathological analysis after IV administration of DOX (15mg/kg) on 7 days after last dose resulted in loss of myocardial tissue, focal necrosis of muscle fibers with

eosinophilia in the cytoplasm, disarray and destruction of muscle fibers with focal hemorrhage (Figure 6.10B). However, PolyDOX (20mg/kg) treated group on 21 days exhibit relatively normal myocardial cells with vascular dilatation and reasonable degeneration of some fibril cells (Figures 6.10C), compared to the control (Figure 6.10A). Histological changes were also found in the liver of DOX (15mg/kg) treated group as compared to both control and PolyDOX (20mg/kg) (Figure 6.10E). DOX (15mg/kg) treated mice showed diffuse fatty degeneration and necrotic changes in the liver (Figure 6.10E). PolyDOX (20mg/kg) treated mice showed similar change, but all were milder than DOX (15mg/kg) treated mice (Figure 6.10F). There were no significant abnormalities observed in the other organ tissues treated with PolyDOX.

Table 6.9 Serum biochemistry in healthy BalB/c mice on day 7 and 21 after last intravenous doses of PolyDOX injections (5mg/kg/day), (4×5mg/kg/day), (3×5mg/kg/day), free DOX injections (3×5mg/kg/day), (5mg/kg/day) and Polymersomes (20mg/kg/day)

Parameter (Units)	Days	Untreated (Control)	DOX (5mg/kg)	PolyDOX (5mg/kg)	Blank-POLY (20mg/kg)	DOX (15mg/kg	PolyDOX (15mg/kg)	PolyDOX (20mg/kg)
CPK (IU/l)	7	97±13.5	184±12.7	103±9.6	96±21.1	349±24.7	118±14.7	121±13.8
	21	112±25.7	173±11.5	98±12.9	101±16.2		114±9.1	117±21.5
LDH (IU/l)	7	376±33.9	646±51.7	384±41.6	381±50.2	796±53.7	393±43.7	401±23.1
	21	389±31.7	546±39.1	392±36.2	397±38.7		386±29.4	391±29.1
ALT (IU/l)	7	32.8±2.82	61.1±3.92	37.9±2.40	33.7±3.2	89.4±1.82	41.6±2.46	39.1±2.97
	21	34.1±1.73	71.9±4.41	42.4±3.12	31.4±2.97		44.1±3.52	47.8±2.57
AST (IU/l)	7	64.9±2.97	129±8.27	69.3±5.71	60.4±3.29	184±2.82	79.2±4.27	82.4±7.16
	21	69.7±4.11	137±4.29	71.3±4.93	64.2±1.12		81.4±6.51	80.±3.19
Creatine mg/dl	7	0.78±0.103	1.1± 0.08	0.84±0.05	0.71±0.02	1.68±0.07	0.87±0.1	0.92±0.03
	21	0.81±0.03	1.07±0.01	0.81±0.11	0.79±0.06		0.91±0.02	0.94±0.07
BUN mg/dl	7	18.6±1.40	23.6±1.71	21.1±2.01	19.4±1.75	42.7±2.69	21.4±1.32	24.1±2.29
	21	21.4±2.17	25.2±1.92	23.7±2.14	21.9±1.94		25.1±2.74	26.2±1.85

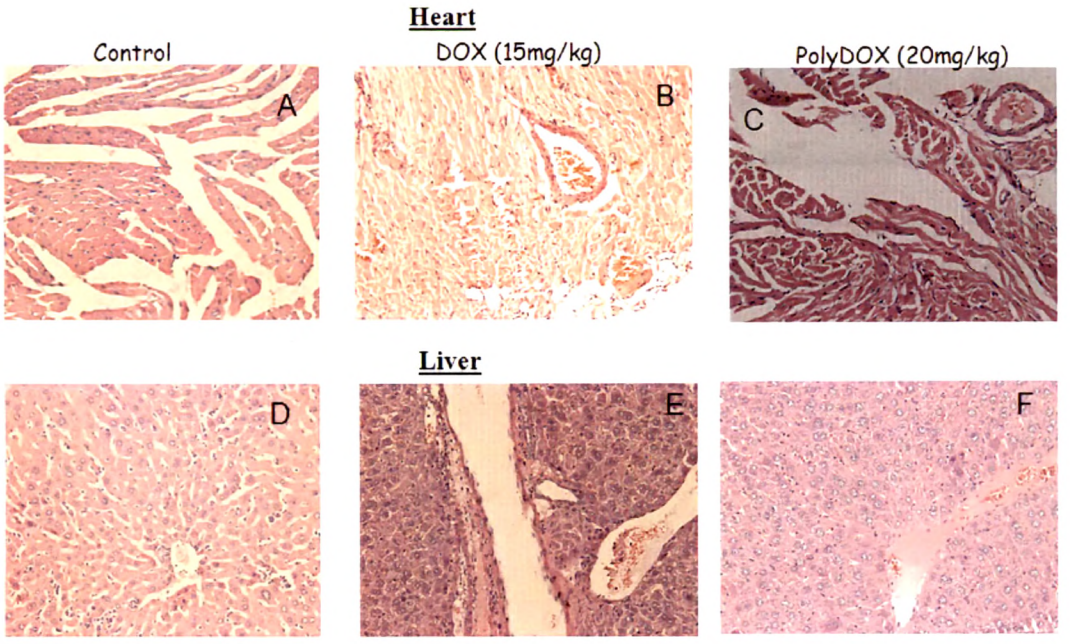

Figure 6.10 Photo micrograph of heart tissues (A-C) and liver tissues (D-F) after treatment with Saline (A, D), DOX (15mg/kg) (B, E) and PolyDOX (20mg/kg) (C, F).

6.15.7. *Hemolysis effect of PolyDOX and Blank-POLY*

Hemolytic profile is presented in Figure 6.11 of PolyDOX and Blank-POLY at different concentration. It is clear from profiles that Blank-POLY did not show hemolytic activity even at high concentration (500µg/mL). However, slight hemolysis (approximately 4%) was observed in case of PolyDOX. PolyDOX could release DOX in experimental conditions because it releases DOX ~ 30% in 1h at 37°C *in vitro* (Upadhyay et al., 2009). Therefore, the leakage of hemoglobin from the RBC could be attributed to the action of released DOX on the cell membranes. Free DOX has been reported for 11% hemolytic activity at 200µg/mL in similar experimental conditions (Shuai et al., 2004). It is known that interaction between RBC and particles depends on the surface charge of the particles and for hemolytic activity the sequence is, cationic charge particle > anionic charge particle > neutral charge particle. Therefore, presence of hyaluronan (anionic charges polymer) on PolyDOX hinder the interaction between RBC and Blank-POLY or PolyDOX. In addition, it has been demonstrated that interaction between RBC and charged particles also depends on the softness or hydrophilicity of the surface of the particle instead of charge (Makino et al., 1999; He et al., 2009). The presence of

hydrophilic hyaluronan on the polymersomes provides hydrophilic or soft surface which could also prevent contacting with the RBC and suppress the hemolytic activity of encapsulated drug. Currently, some low molecular weight surfactants such as Tween 80, used in IV administration of hydrophobic drugs, have been reported to interact with cell membrane of RBC and cause significant hemolytic activity (Cheon Lee et al., 2003). Therefore PolyDOX are apparently more hemocompatible compared to these low molecular weight surfactants in drug delivery.

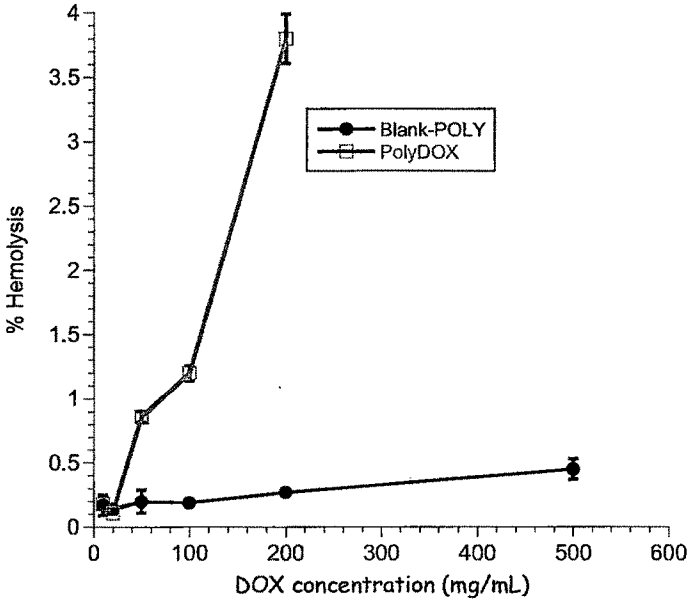

Figure 6.11 Hemolytic activities of the PolyDOX and Blank-POLY. Each data was repeated three times to provide the standard deviation (n=3).

6.15.8. *Antitumor activity of PolyDOX and DOX*

In vivo animal studies were carried out to examine targeting and anti-tumor effects of PolyDOX using a EAT bearing BalB/c mice model. Figure 6.12A shows the progress of tumor volume growth observed for 30 days after treatment with free DOX and PolyDOX at 5mg/kg body weight dose equivalent to DOX. PolyDOX suppressed the tumor growth significantly ($P < 0.01$) then control (Figure 6.12 A). PolyDOX dominantly control tumor growth compared to free DOX ($P<0.01$) as seen in figure 6.12B which demonstrate percent relative tumor inhibition of free DOX and PolyDOX compared to control. In addition we also determined efficacy of PolyDOX as by calculating tumor volume

doubling time (DT). Polydox significantly (P<0.01) delay doubling time of EAT tumor compare to control and DOX treated group whereas no difference (P >0.05) in doubling time of EAT tumor between free DOX and control group animals (Figure 6.13).

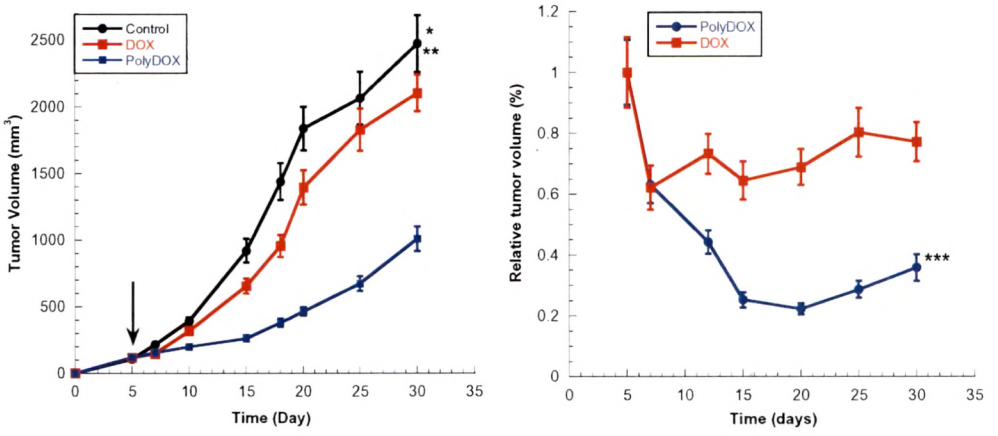

Figure 6.12 (A) Tumor growth inhibition by single injection of DOX and PolyDOX at 5mg/kg dose in EAT tumor-bearing BalB/c mice. Injected PBS solution was considered as a control treatment. The arrow indicates the number of days after the implantation of the EAT cells on that the formulations were injected. (B) Represent the relative tumor growth after administration of DOX and PolyDOX compared to control. (*P < 0.01 vs. PolyDOX, **P > 0.05 vs. DOX, ***P < 0.01 vs. DOX). The data represent the mean of six animals±SD.

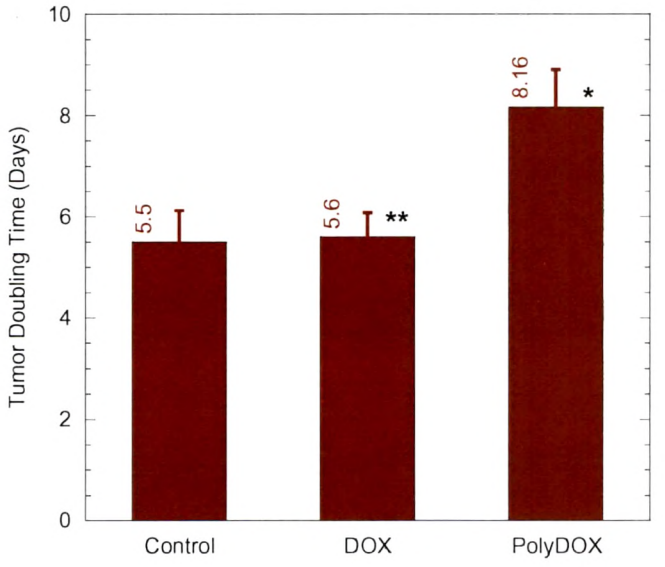

Figure 6.13 Tumor volume doubling time (DT) of EAT tumor bearing mice treated with free DOX and PolyDOX at 5mg/kg equivalent to free DOX. (*P < 0.01 vs. DOX, *P < 0.01 vs. control, **P > 0.05 vs. control). The data represent the mean of six animals ± SD.

Two mechanisms could be involved in antitumor effect of PolyDOX which is passive targeting and active targeting. Passive targeting of nanoparticles is also known as "enhanced permeation and retention" (EPR) effect, is attributed to the presence of leaky tumor vessels and less effective lymphatic drainage system in tumors (Maeda et al., 1992, 2009). Accumulation of circulating macromolecules and nanoparticles in tumor mainly depends on their molecular weight and particle size (Dreher et al., 2006). Subcutaneously grown tumor can exhibit a characteristic pore cutoff size ranging from 200 nm to 1.2μm (Hobbs et al., 1998) and sterically stabilized liposomes of 400 nm in diameter were able to penetrate into tumor interstitium (Yuan et al., 1995). Choi et al., 2009 had also found that hyaluronan nanoparticles (400nm) were successfully accumulated in the tumor tissue owing to the nanoparticle's EPR effect in tumor-bearing mice. In addition, passively targeted PolyDOX that were accumulated in the EAT tumor region might be more readily taken up by tumor cells by a CD44 receptor-mediated endocytosis process (active targeting) because EAT cells are significantly ($P<0.001$) positive for CD44 receptor (Figure 6.4). PolyDOX having a size of about ~400nm were likely to extravasate through the endothelial junctions of the leaky blood vessels in tumor tissue, but not in normal tissue. Therefore, in biodistribution results PolyDOX uptake in muscles is less compared to tumor uptake ($P<0.05$). A combined effect of the passive targeting and active targeting would be the main reason for the suppression of tumor growth in case of PolyDOX. We had also observed the survival time of treated EAT tumor bearing mice and drawn Kaplan-Meier survival curve (Figure 6.14 A). We continued to observe the survival of mice till tumor volume reach 50% above than ethical limit ($2000mm^3$) (Greeneltch et al., 2007) or death occurred after post treatments. PolyDOX increased survival time compared to control and free DOX. PolyDOX treated mice was able to survive for more than 2.5 months (Figure 6.14A). We calculated Increase in Life Span (ILS) from the survival data and plotted (Figure 6.14B). PolyDOX increases ILS 6 times more than free DOX. It is rational to expect that the higher DOX levels of the PolyDOX in the tumor would result in higher therapeutic potency.

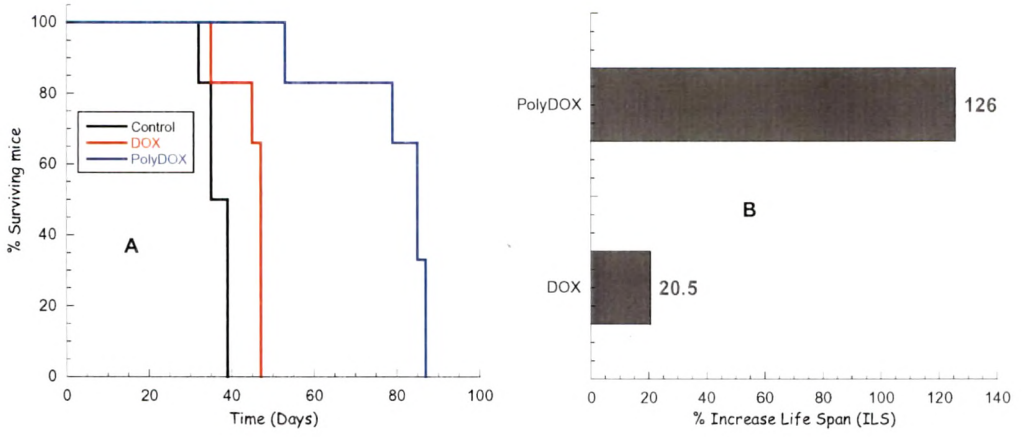

Figure 6.14 (A) Kaplan-Meier survival curve of mice treated with DOX and PolyDOX, (B) % Increase in Life Span (ILS) of mice treated with DOX and PolyDOX compared to control. PolyDOX treated groups survived significantly longer as compared to control and DOX ($P<0.001$).

6.15.9. *Gamma Scintigraphy study*

The use of gamma ray emitting radionucleotide (^{99m}Tc) enabled us to perform imaging studies to visual proof of ^{99m}Tc-PolyDOX uptake in tumor. Imaging of animals was carried out at different time intervals (1, 4 and 6h) after administering labeled compound intravenously at 5mg/kg body weight dose equivalent to DOX. Scintigraphic images showed rapid accumulation of radioactivity in major organs (liver, spleen and lungs) after IV injection of ^{99m}Tc-PolyDOX in EAT tumor bearing BalB/c mice. It was difficult to record counts in separate organs and to get images in small animals because of more uptakes of PolyDOX in major organs. But still, it can be attested from the images (Figure 6.15) that PolyDOX was accumulated in tumor as indicated by the arrow.

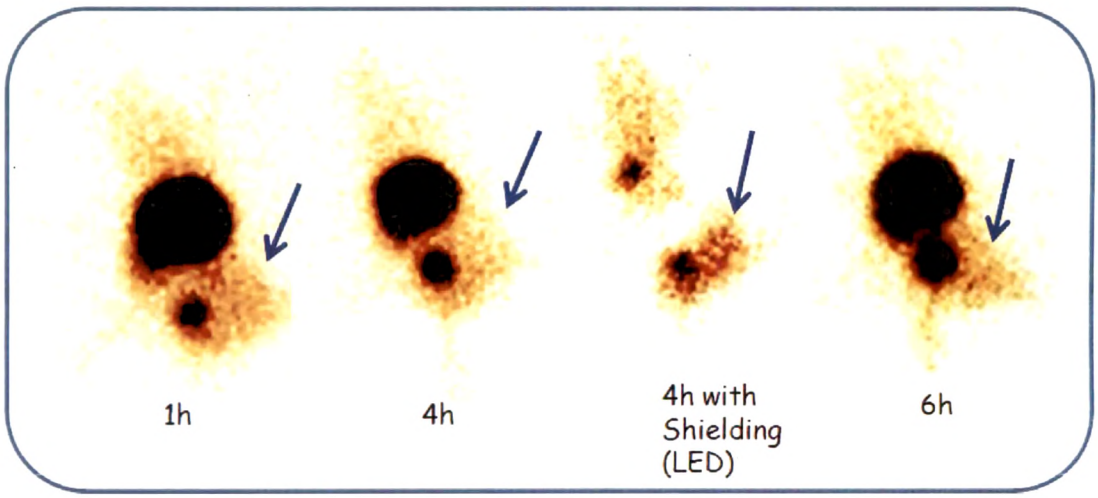

Figure 6.15 Gamma Scintigraphy of BalB/c mouse bearing Ehrich Ascites Tumor (EAT) in the right thigh after intravenous administration of 100 µCi ^{99m}Tc-PolyDOX. The arrow indicates the accumulation of ^{99m}Tc-PolyDOX at the tumor site at different time.

6.16. Conclusion

^{99m}Tc labeled compounds (DOX, PolyDOX and Blank-POLY) were prepared by a direct method with more than 99% radiolabeling efficiency. Labeled compounds were stable *in vitro, in vivo* and against DTPA challenge. Blood circulation ($t_{1/2}$) and mean residence time (MRT) had increased for PolyDOX compared to free DOX. Biodistribution data demonstrated that PolyDOX were successfully accumulated at the tumor tissue owing to the passive accumulation (EPR effect) and active targeting (CD44 mediated endocytosis) in EAT bearing mice. In addition, undesirable and higher liver accumulation of PolyDOX doesn't effect significantly hematology parameters and serum enzymes levels and also did not show significant difference in histopathology examination of tissue compared to control. PolyDOX suppress EAT tumor growth and Increase in Life Span (ILS) of tumor bearing mice compared to control and free DOX. Gama scintigraphy images illustrates accumulation of ^{99m}Tc-PolyDOX in EAT tumor of mice.

References

- Agashe HB, Babbar AK, Jain S, Sharma RK, Mishra AK, Asthana A, Garg M, Dutta T, Jain NK. Investigations on biodistribution of technetium-99m-labeled carbohydrate-coated poly(propylene imine) dendrimers. Nanomedicine 2007;3(2):120-7.

- Ahmed F, Pakunlu RI, Srinivas G, Brannan A, Bates F, Klein ML, Minko T, Discher DE. Shrinkage of a rapidly growing tumor by drug-loaded polymersomes: pH-triggered release through copolymer degradation. Mol Pharm 2006;3(3):340-50.
- Arulsudar N, Subramanian N, Mishra P, Chuttani K, Sharma RK, Murthy RS. Preparation, characterization, and biodistribution study of technetium-99m-labeled leuprolide acetate-loaded liposomes in ehrlich ascites tumor-bearing mice. AAPS J 2004;6(1):45-56.
- Auzenne E, Ghosh SC, Khodadadian M, Rivera B, Farquhar D, Price RE, Ravoori M, Kundra V, Freedman RS, Klostergaard J. Hyaluronic acid-paclitaxel: antitumor efficacy against CD44(+) human ovarian carcinoma xenografts. Neoplasia 2007;9(6):479-86.
- Bae Y, Nishiyama N, Fukushima S, Koyama H, Yasuhiro M, Kataoka K. Preparation and biological characterization of polymeric micelle drug carriers with intracellular pH-triggered drug release property: tumor permeability, controlled subcellular drug distribution, and enhanced in vivo antitumor efficacy. Bioconjug Chem 2005;16(1):122-30.
- Banzato A, Bobisse S, Rondina M, Renier D, Bettella F, Esposito G, Quintieri L, Meléndez-Alafort L, Mazzi U, Zanovello P, Rosato A. A paclitaxel-hyaluronan bioconjugate targeting ovarian cancer affords a potent in vivo therapeutic activity. Clin Cancer Res 2008;14(11):3598-606.
- Banzato A, Rondina M, Meléndez-Alafort L, Zangoni E, Nadali A, Renier D, Moschini G, Mazzi U, Zanovello P, Rosato A. Biodistribution imaging of a paclitaxel-hyaluronan bioconjugate. Nucl Med Biol 2009;36(5):525-33.
- Bao A, Goins B, Klipper R, Negrete G, Phillips WT. Direct 99mTc labeling of pegylated liposomal doxorubicin (Doxil) for pharmacokinetic and non-invasive imaging studies. J Pharmacol Exp Ther 2004;308(2):419-25.
- Cheon Lee S, Kim C, Chan Kwon I, Chung H, Young Jeong S. Polymeric micelles of poly(2-ethyl-2-oxazoline)-block-poly(epsilon-caprolactone) copolymer as a carrier for paclitaxel. J Control Release 2003;89(3):437-46.

- Choi KY, Min KH, Na JH, Choi K, Kim K, Park JH, Kwon IC, Jeong SY. Self-assembled hyaluronic acid nanoparticles as a potential drug carrier for cancer therapy: Synthesis, characterization, and in vivo biodistribution. Journal of Materials Chemistry 2009;19(24)4102-07.
- Coradini D, Zorzet S, Rossin R, Scarlata I, Pellizzaro C, Turrin C, Bello M, Cantoni S, Speranza A, Sava G, Mazzi U, Perbellini A. Inhibition of hepatocellular carcinomas in vitro and hepatic metastases in vivo in mice by the histone deacetylase inhibitor HA-But. Clin Cancer Res 2004;10(14):4822-30.
- Devalapally H, Duan Z, Seiden MV, Amiji MM. Paclitaxel and ceramide co-administration in biodegradable polymeric nanoparticulate delivery system to overcome drug resistance in ovarian cancer. Int J Cancer 2007;121(8):1830-8.
- Discher DE, Eisenberg A. Polymer vesicles. Science 2002;297(5583):967-73.
- Dobrovolskaia MA, Clogston JD, Neun BW, Hall JB, Patri AK, McNeil SE. Method for analysis of nanoparticle hemolytic properties in vitro. Nano Lett 2008; 8(8):2180-7.
- Dong X, Mattingly CA, Tseng MT, Cho MJ, Liu Y, Adams VR, Mumper RJ. Doxorubicin and paclitaxel-loaded lipid-based nanoparticles overcome multidrug resistance by inhibiting P-glycoprotein and depleting ATP. Cancer Res 2009;69(9):3918-26.
- Dreher MR, Liu W, Michelich CR, Dewhirst MW, Yuan F, Chilkoti A. Tumor vascular permeability, accumulation, and penetration of macromolecular drug carriers. J Natl Cancer Inst 2006;98(5):335-44.
- ElBayoumi TA, Torchilin VP. Tumor-targeted nanomedicines: enhanced antitumor efficacy in vivo of doxorubicin-loaded, long-circulating liposomes modified with cancer-specific monoclonal antibody. Clin Cancer Res 2009;15(6):1973-80.
- Ferreira E, da Silva AE, Serakides R, Gomes MG, Cassali GD. Ehrlich tumor as model to study artificial hyperthyroidism influence on breast cancer. Pathol Res Pract 2007;203(1):39-44.

- Greeneltch KM, Schneider M, Steinberg SM, Liewehr DJ, Stewart TJ, Liu K, Abrams SI. Host immunosurveillance controls tumor growth via IFN regulatory factor-8 dependent mechanisms. Cancer Res 2007;67(21):10406-16.
- Greish K, Sawa T, Fang J, Akaike T, Maeda H. SMA-doxorubicin, a new polymeric micellar drug for effective targeting to solid tumours. J Control Release 2004;97(2):219-30.
- Han HD, Lee A, Song CK, Hwang T, Seong H, Lee CO, Shin BC. In vivo distribution and antitumor activity of heparin-stabilized doxorubicin-loaded liposomes. Int J Pharm 2006;313(1-2):181-8.
- Harada A, Kataoka K. Supramolecular assemblies of block copolymers in aqueous media as nanocontainers relevant to biological applications. Progress in Polymer Science 2006;31(11)949-82,
- Harivardhan Reddy L, Sharma RK, Chuttani K, Mishra AK, Murthy RS. Influence of administration route on tumor uptake and biodistribution of etoposide loaded solid lipid nanoparticles in Dalton's lymphoma tumor bearing mice. J Control Release 2005;105(3):185-98.
- Harris EN, Kyosseva SV, Weigel JA, Weigel PH. Expression, processing, and glycosaminoglycan binding activity of the recombinant human 315-kDa hyaluronic acid receptor for endocytosis (HARE). J Biol Chem 2007;282(5):2785-97.
- He M, Zhao Z, Yin L, Tang C, Yin C. Hyaluronic acid coated poly(butyl cyanoacrylate) nanoparticles as anticancer drug carriers. Int J Pharm 2009;373(1-2):165-73.
- Hobbs SK, Monsky WL, Yuan F, Roberts WG, Griffith L, Torchilin VP, Jain RK. Regulation of transport pathways in tumor vessels: role of tumor type and microenvironment. Proc Natl Acad Sci USA 1998;95(8):4607-12.
- Huynh NT, Passirani C, Saulnier P, Benoit JP. Lipid nanocapsules: A new platform for nanomedicine. Int J Pharm 2009 May 3 (Inpress).

- Ishida T, Shiraga E, Kiwada H. Synergistic antitumor activity of metronomic dosing of cyclophosphamide in combination with doxorubicin-containing PEGylated liposomes in a murine solid tumor model. J Control Release 2009;134(3):194-200.
- Ito T, Muraoka S, Takahashi K, Fujio Y, Schaffer SW, Azuma J. Beneficial effect of taurine treatment against doxorubicin-induced cardiotoxicity in mice. Adv Exp Med Biol 2009;643:65-74.
- Jannin V, Musakhanian J, Marchaud D. Approaches for the development of solid and semi-solid lipid-based formulations. Adv Drug Deliv Rev 2008;60(6):734-46.
- Kataoka K, Harada A, Nagasaki Y. Block copolymer micelles for drug delivery: Design, characterization and biological significance, Adv Drug Deliv Rev 200;47(1):113-31.
- Kim Y, Tewari M, Pajerowski JD, Cai S, Sen S, Williams J, Sirsi S, Lutz G, Discher DE.Polymersome delivery of siRNA and antisense oligonucleotides. J Control Release 2009;134(2):132-40.
- Levine DH, Ghoroghchian PP, Freudenberg J, Zhang G, Therien MJ, Greene MI, Hammer DA, Murali R. Polymersomes: a new multi-functional tool for cancer diagnosis and therapy. Methods 2008;46(1):25-32.
- Liu S, Edwards DS, Barrett JA. ^{99m}Tc labeling of highly potent small peptides. Bioconjug Chem 1997;8(5):621-36.
- Luo Y, Ziebell MR, Prestwich GD. A hyaluronic acid-taxol antitumor bioconjugate targeted to cancer cells. Biomacromolecules 2000;1(2):208-18.
- Maeda H, Bharate GY, Daruwalla J. Polymeric drugs for efficient tumor-targeted drug delivery based on EPR-effect. Eur J Pharm Biopharm 2009;71(3):409-19.
- Maeda H, Seymour LW, Miyamoto Y. Conjugates of anticancer agents and polymers: advantages of macromolecular therapeutics in vivo. Bioconjug Chem 1992;3(5):351-62.
- Makino K, Umetsu M, Goto Y, Nakayama A, Suhara T, Tsujii J, Kikuchi A, Ohshima H, Sakurai Y, Okano T. Interaction between charged soft microcapsules and red

blood cells: Effects of PEGylation of microcapsule membranes upon their surface properties . Colloids and Surfaces B: Biointerfaces 1999;13(6)287-97.

- Meléndez-Alafort L, Riondato M, Nadali A, Banzato A, Camporese D, Boccaccio P, Uzunov N, Rosato A, Mazzi U. Bioavailability of 99mTc-Ha-paclitaxel complex [99mTc-ONCOFID-P] in mice using four different administration routes. Journal of Labelled Compounds and Radiopharmaceuticals 2006;49(11)939-50.
- Minko T, Pakunlu RI, Wang Y, Khandare JJ, Saad M. New generation of liposomal drugs for cancer. Anticancer Agents Med Chem 2006;6(6):537-52.
- Mishra AK, Iznaga-Escobar N, Figueredo R, Jain VK, Dwarakanath BS, Pérez-Rodríguez R, Sharma RK, Mathew TL. Preparation and comparative evaluation of ^{99m}Tc-labeled 2-iminothiolane modified antibodies and CITC-DTPA immunoconjugates of anti-EGF-receptor antibodies. Methods Find Exp Clin Pharmacol 2002; 24(10):653-60.
- Moghimi SM, Hedeman H, Muir IS, Illum L, Davis SS. An investigation of the filtration capacity and the fate of large filtered sterically-stabilized microspheres in rat spleen. Biochim Biophys Acta 1993;1157(3):233-40.
- Nakanishi T, Fukushima S, Okamoto K, Suzuki M, Matsumura Y, Yokoyama M, Okano T, Sakurai Y, Kataoka K. Development of the polymer micelle carrier system for doxorubicin. J Control Release 2001;74(1-3):295-302.
- Panwar P, Singh S, Kumar N, Rawat H, Mishra AK. Synthesis, characterization, and in vivo skeletal localization of a new ^{99m}Tc-based multidentate phosphonate chelate: 5-Amino-1,3-bis(ethylamine-(N,N dimethyl diphosphonic acid) acetamido) benzene. Bioorganic and Medicinal Chemistry 2007;15(2)1138-45.
- Peer D, Margalit R. Loading mitomycin C inside long circulating hyaluronan targeted nano-liposomes increases its antitumor activity in three mice tumor models. Int J Cancer 2004a;108(5):780-9.

- Peer D, Margalit R. Tumor-targeted hyaluronan nanoliposomes increase the antitumor activity of liposomal Doxorubicin in syngeneic and human xenograft mouse tumor models. Neoplasia 2004b;6(4):343-53.
- Phillips WT, Klipper RW, Awasthi VD, Rudolph AS, Cliff R, Kwasiborski V, Goins BA. Polyethylene glycol-modified liposome-encapsulated hemoglobin: a long circulating red cell substitute. J Pharmacol Exp Ther 1999;288(2):665-70.
- Platt VM, Szoka FC Jr. Anticancer therapeutics: Targeting macromolecules and nanocarriers to hyaluronan or CD44, a hyaluronan receptor. Mol Pharm 2008;5(4):474-86.
- Rosato A, Banzato A, De Luca G, Renier D, Bettella F, Pagano C, Esposito G, Zanovello P, Bassi P. HYTAD1-p20: a new paclitaxel-hyaluronic acid hydrosoluble bioconjugate for treatment of superficial bladder cancer. Urol Oncol 2006; 24(3):207-15.
- Saha GB. Fundamentals of Nuclear Pharmacy. Fifth Edition. 2004. Springer-Verlag New York, Inc., US.
- Shuai X, Ai H, Nasongkla N, Kim S, Gao J. Micellar carriers based on block copolymers of poly(epsilon-caprolactone) and poly(ethylene glycol) for doxorubicin delivery. J Control Release 2004;98(3):415-26.
- Sugahara S, Okuno S, Yano T, Hamana H, Inoue K. Characteristics of tissue distribution of various polysaccharides as drug carriers: influences of molecular weight and anionic charge on tumor targeting. Biol Pharm Bull 2001;24(5):535-43.
- Upadhyay K, Agrawal H, Upadhyay C, Schatz C, Le Meins J, Misra A, Lecommandoux S. Role of block copolymer nanoconstructs in cancer therapy. Crit Rev Ther Drug Carrier Syst 2009a;26(2):157-205.
- Upadhyay KK, Meins JF, Misra A, Voisin P, Bouchaud V, Ibarboure E, Schatz C, Lecommandoux S. Biomimetic Doxorubicin Loaded Polymersomes from Hyaluronan-block-Poly(gamma-benzyl glutamate) Copolymers. Biomacromolecules 2009b; Aug 5 (on Web).

- Vyas TK, Babbar AK, Sharma RK, Singh S, Misra A. Intranasal mucoadhesive microemulsions of clonazepam: preliminary studies on brain targeting. J Pharm Sci 2006; 95(3):570-80.
- Wang JP, Maitani Y, Takayama K, Nagai T. Pharmacokinetics and antitumor effect of doxorubicin carried by stealth and remote loading proliposome. Pharm Res 2000;17(7):782-7.
- Wu MS, Robbins JC, Bugianesi RL, Ponpipom MM, Shen TY. Modified in vivo behavior of liposomes containing synthetic glycolipids. Biochim Biophys Acta 1981;674(1):19-29.
- Xu Z, Chen L, Gu W, Gao Y, Lin L, Zhang Z, Xi Y, Li Y. The performance of docetaxel-loaded solid lipid nanoparticles targeted to hepatocellular carcinoma. Biomaterials 2009;30(2):226-32.
- Yadav AK, Mishra P, Mishra AK, Mishra P, Jain S, Agrawal GP. Development and characterization of hyaluronic acid-anchored PLGA nanoparticulate carriers of doxorubicin. Nanomedicine 2007;3(4):246-57.
- Yokoyama M, Fukushima S, Uehara R, Okamoto K, Kataoka K, Sakurai Y, Okano T. Characterization of physical entrapment and chemical conjugation of adriamycin in polymeric micelles and their design for in vivo delivery to a solid tumor. J Control Release 1998;50(1-3):79-92.
- Yuan F, Dellian M, Fukumura D, Leunig M, Berk DA, Torchilin VP, Jain RK. Vascular permeability in a human tumor xenograft: molecular size dependence and cutoff size. Cancer Res 1995;55(17):3752-6.
- Zhou B, Weigel JA, Fauss L, Weigel PH. Identification of the hyaluronan receptor for endocytosis (HARE). J Biol Chem 2000;275(48):37733-41.